

Statistics of Lyapunov exponent in one-dimensional layered systems

Pi-Gang Luan and Zhen Ye

Wave Phenomena Laboratory, Department of Physics, National Central University, Chung-li, Taiwan 32054
(October 24, 2018)

Localization of acoustic waves in a one dimensional water duct containing many randomly distributed air filled blocks is studied. Both the Lyapunov exponent and its variance are computed. Their statistical properties are also explored extensively. The results reveal that in this system the single parameter scaling is generally inadequate no matter whether the frequency we consider is located in a pass band or in a band gap. This contradicts the earlier observations in an optical case. We compare the results with two optical cases and give a possible explanation of the origin of the different behaviors.

PACS numbers: 42.25.Dd, 89.75.Da

I. INTRODUCTION

The fact that the electronic localization in disordered systems [1] is of wave nature has led to suggestion that classical waves could be similarly localized in random systems. The effort in searching for localization of classical waves such as acoustic and electro-magnetic waves is tremendous. It has drawn intensive attentions from both theorists [2–8] and experimentalists [9,10]. Since the pioneering work of Anderson et.al. [11], the concepts of universality and scaling have become important [12–16]. These ideas stem from the insensitivity of the macroscopic laws to microscopic details; that is, systems or models which differ from each other on a microscopic level can show identical macroscopic behavior. According to the hypothesis of single-parameter scaling (SPS) [11,15,16], if the localization behaviors of a 1D disordered system obey SPS, the Lyapunov exponent or inverse localization that characterizes the degree of localization will be proportional to its variance.

In a recent study of acoustic (AC) waves propagation in a one dimensional randomly layered system [17] we have found that the statistics relation between Lyapunov exponent (LE) γ and its variance $\text{var}(\gamma)$ do not follow the predictions of single parameter scaling (SPS). However, in an earlier study on 1D localization behaviors of electro-magnetic (EM) waves [15], the author claimed that the non-universal behaviors of LE will disappear and SPS will be restarted while the randomness of the system exceeds a critical value. Since for 1D propagation the AC and EM waves are in fact mathematically equivalent, i.e., there exists one to one correspondence between these two kinds of waves, it looks quite impossible that they can have different localization behaviors. In order to understand where do the main differences between these two kinds of models come from, in this paper we study EM and AC systems simultaneously. Two EM models and one AC model are studied in this paper. We find that though the statements made by Deych et.al. [15] are correct in their chosen case, however, the applicability of SPS is more or less based on the fact that the impedance

contrast between the constituents of the wave media is closed to 1. Without this restriction then even in the EM systems SPS will not be restored in the high randomness limit.

This paper is organized as follows. In the next section we explain the correspondence between EM and AC waves and define the three models employed in this paper. In Sec. III we first review the previous results and then discuss the numerical results of the three chosen models. A possible explanation of the origin of the novel properties of the AC localization are also proposed. Concluding remarks are given in section IV.

II. THEORY AND MODELS

To begin with, we explain the one to one correspondence of the 1D propagation between AC and EM waves. For simplicity while without destroying the generality we restrict our discussion to the monochromatic waves with time dependence $e^{-i\omega t}$. We also assume that waves are normally incident on the left boundary of the media and propagate along the x-axis. The 1D propagation of AC waves under these assumptions is governed by

$$\frac{d}{dx} \left(\frac{1}{\rho} \frac{dp}{dx} \right) = -\frac{\omega^2 p}{\rho c^2} \quad (1)$$

where $\rho = \rho(x)$, $p = p(x)$ and $c = c(x)$ represent the mass density, the pressure, and the phase velocity of the wave in the media, respectively. In the special case of layered media considered in [17], ρ and c are all constants in a single layer. Across an interface that separate two layers either ρ or c jump to a different value but pressure p and media vibration velocity

$$u = \frac{1}{i\omega\rho} \frac{dp}{dx} \quad (2)$$

must be continuously connected. The continuity conditions for every interfaces together with the wave equation (1) itself determine the dynamics of the whole system.

Similarly, the equation governing 1D propagation of monochromatic EM waves can be deduced from Maxwell equation and is written as

$$\frac{d}{dx} \left(\frac{1}{\mu} \frac{dE}{dx} \right) = -\frac{\omega^2 \epsilon E}{c_0^2} = -\frac{\omega^2 E}{\mu c^2} \quad (3)$$

or

$$\frac{d}{dx} \left(\frac{1}{\epsilon} \frac{dH}{dx} \right) = -\frac{\omega^2 \mu H}{c_0^2} = -\frac{\omega^2 H}{\epsilon c^2}, \quad (4)$$

where $E = E_y$ and $H = H_z$ are the electric and magnetic fields, ϵ and μ stand for the permittivity and permeability, c_0 is the speed of light in vacuum and $c = c_0/\sqrt{\epsilon\mu}$ is the speed of light in the media. Comparing Eq. (3) and (4) with Eq. (1) one can easily recognize the equivalence between AC and EM models via the substitutions

$$E \rightarrow p, \quad H \rightarrow -u, \quad \epsilon \rightarrow 1/\rho c^2, \quad \mu \rightarrow \rho \quad (5)$$

in Eq. (3) or

$$H \rightarrow p, \quad E \rightarrow u, \quad \epsilon \rightarrow \rho, \quad \mu \rightarrow 1/\rho c^2 \quad (6)$$

in Eq. (4).

In spite of these similarities, the two models discussed in [17] and [15] indeed have some different features. First, in the optical case that described in Eq. (3), one usually assumes $\mu = 1$. However, in our AC model the corresponding quantity is ρ . The mass density ratio between water and air is about 775, a very large value. Second, the phase velocity ratio in our model is 4.455, whereas in [15] the ratio is 1.0945. Third, the thickness ratio in our model is 9999/1, much larger than 1/1 that considered in [15]. Fourth, we randomize the thickness of the water layers (medium with high phase velocity) and keep the thickness of air layers (medium with low phase velocity) constant. In [15] they randomize the thickness of the layers with low phase velocity.

To clarify where do the major differences come from, we define three models and study them numerically. The system for each model is a composite made of two kinds of material A and B with corresponding thickness a_j and b_j in the j th A/B layer. For simplicity hereafter we assume $a_j = a$, i.e., all A type layers have the same size. Any quantity Q in A and B type layers are denoted as Q_a and Q_b respectively.

- Model 1 is an optical model with $\epsilon_b/\epsilon_a = 2$ and $\mu_b/\mu_a = 1$. The thickness ratio is $\langle b \rangle/a = 1$, where $b \in \langle b \rangle[1 - \Delta, 1 + \Delta]$ and $\Delta \in [0, 1]$.
- Model 2 is also an optical model with $\epsilon_b/\epsilon_a = 20$ and $\mu_b/\mu_a = 1$. The thickness ratio is $\langle b \rangle/a = 1$, where $b \in \langle b \rangle[1 - \Delta, 1 + \Delta]$ and $\Delta \in [0, 1]$.
- Model 3 is our previously considered acoustic model with $c_b/c_a = 4.455$ and $\rho_b/\rho_a = 755.2$. The thickness ratio is given by $\langle b \rangle/a = 9999$, where $b \in \langle b \rangle[1 - \Delta, 1 + \Delta]$ and $\Delta \in [0, 1]$.

In a single layer the impedance of AC waves is given by ρc and the impedance of EM waves is given by ϵc or μc . Thus we see that in Model 3 the impedance contrast is about 3365 and impedance contrast in Model 1 and 2 are about 1.414 and 4.472 respectively.

III. NUMERICAL RESULTS

Before the discussion of the numerical results we first summarize the relevant results of our previous study [17]. There both LE and its variance as functions of frequency were studied. At low disorders, the variance of LE inside the gaps is small. Contrast to the optical case [15], there are no double maxima inside the gap. With increasing disorder, double peaks appears inside the allowed bands. When exceeding a certain critical value, however, the double peaks emerge. The higher frequency, the lower is the critical value. The increasing disorder reduces the band gap effect and smears LE. We also plotted LE-variance relations. However, with increasing disorder, we did not observe linear dependence between LE and its variance, as expected from the single parameter scaling theory.

Now we turn to the discussion of the three chosen models. When randomness $\Delta = 0$, the layered systems become periodic. Eigenfunctions of wave equation in a periodic environment are Bloch waves. As is well known, band structure appears in this situation. The understanding of band structure is very important and helpful in the following discussions. The dispersion relation of the Bloch waves in the underlying periodic system is given by

$$\cos Kd = \cos k_a a \cos k_b b - \cosh 2\eta \sin k_a a \sin k_b b \quad (7)$$

with $d = a + b$ representing the thickness of the space period and K the Bloch wave number. Here for model 1 and 2 function $\cosh 2\eta$ is defined as

$$\cosh 2\eta = \frac{1}{2} \left(\sqrt{\frac{\epsilon_b}{\epsilon_a}} + \sqrt{\frac{\epsilon_a}{\epsilon_b}} \right) \quad (8)$$

and for model 3 it is given by

$$\cosh 2\eta = \frac{1}{2} \left(gh + \frac{1}{gh} \right), \quad g = \rho_a/\rho_b, \quad h = c_a/c_b. \quad (9)$$

In the frequency ranges that Kd are real, the waves are freely propagating in the media and by definition the frequency ranges correspond to the pass bands. Beyond the pass bands Kd are not purely real numbers, solutions of wave equation that satisfy appropriate boundary conditions in both the left and right infinity do not exist, and thus the frequency ranges are referred to as the band gaps. If the media is semi-infinite and the periodicity is ended by a boundary, say, the left boundary, then the waves

are localized in the vicinity of the boundary. The penetration depth is equal to $1/|\text{Im}(K)|$. Fig. 1(a1)-(c1) plot the band structures of model 1-3. Solid curves represent $\text{Re}(Kd)$ and cover the pass bands. Broken lines cover the band gaps and represent the inverse penetration depths $\text{Im}(Kd)$. Model 1 has very wide pass bands and very narrow band gaps. Band gaps are wider than pass bands in model 2. Model 3 has very wide band gaps and very narrow pass bands. An important feature of model 3 is that in the band gaps the penetration depth is very small. Even in the first gap (which has the longest penetration depth) the penetration depth is smaller than one period.

To see how randomness influences the transmission properties we select the frequency range that around the second gap and plot the transmission curves on (a2)-(c2). In this calculation 1600 layers (800 periods) are used in model 1 and 200 layers (100 periods) are used in model 2 and 3. In the gaps the transmission rate is almost zero. When randomness is increased we observe that the transmission rate in the pass bands have been reduced much in the model 2 and model 3. On the other hand, the band gaps in model 2 and 3 seem to be more robust than in model 1.

To further explore the influence of randomness we study both LE and its variance. The results are shown in Fig. 2. (A1)-(A5) are results of model 1 and (B1)-(B5) are results of model 2. LE is denoted as γ and its variance is denoted as $\text{var}(\gamma)$. Here γ and $\text{var}(\gamma)$ are defined as

$$\gamma = \lim_{N \rightarrow \infty} \langle \gamma_N \rangle \quad (10)$$

with

$$\gamma_N = \frac{1}{2N} \ln \left(\frac{1}{T_N} \right) \quad (11)$$

and

$$\text{var}(\gamma) = \lim_{N \rightarrow \infty} (\langle \gamma_N^2 \rangle - \langle \gamma_N \rangle^2), \quad (12)$$

here T_N is the transmission rate for system with $2N$ layers (N periods in the corresponding periodic system), and notation $\langle \dots \rangle$ represents the ensemble average. The sample size is chosen in such a way that it is much larger than the localization length and the ensemble average is carried out over 200 random configurations. As expected, when the randomness is small the LE can be approximated by the inverse penetration depth for wave propagating in the underlying semi-infinite periodic system. Like in the case discussed in Ref. [15], the double peaks of $\text{var}(\gamma)$ first appear near the gap edges. The peaks of $\text{var}(\gamma)$ imply the fluctuations of transmission. Further increasing Δ , the $\text{var}(\gamma)$ peaks become fatter and flatter. We observe that if in the vicinity of a peak there is another peak, then increasing the randomness will cause

them to merge. For model 1, as Δ is increased, a pair of $\text{var}(\gamma)$ peaks merge with each other inside the gap, following the scenario of Ref [15]. However, for model 2 when the randomness is increased the pairs of $\text{var}(\gamma)$ peaks tend to merge with each other in the pass bands and finally destroy the pass bands. It seems that in model 2 the merging of the double peaks of $\text{var}(\gamma)$ in a pass band will never be completed. The merging tendency of a pair of double peaks merely increase the LE and destroy the pass band they belong to.

We also plot the LE versus its variance in Fig. 3. There we observe that although for model 1 (with small dielectric contrast between two layers like that studied in [15]) SPS seems still a good approximation in large disorder limit, deviation from SPS is clearly observed in model 2. Similar quantities have also been calculated for model 3 and plotted in Fig. 4 and Fig. 5. There we also observe novel behaviors of γ and $\text{var}(\gamma)$ and find even larger deviation from SPS as reported in [17].

From these observations, we find:

- How does the $\text{var}(\gamma)$ vary with the randomness depends on many parameters. For example, the impedance contrast, the thickness ratio and which kind of layers (for example, high phase velocity, low phase velocity etc.) is randomized.
- When impedance contrast is large, it seems that the deviation from SPS is a usual feature. The results reported in [15] is based more or less on the fact that the impedance contrast between two layers is closed to 1.

In order to understand why the large deviation from SPS in model 3 is established we study its transmission properties in more detail. In Fig. 6(a) we plot the transmission rate of the AC waves through a pair of air blocks of thickness a . The two air blocks are separated by a water layer of thickness $b = 9999a$. Similarly in Fig. 6(b) we plot the transmission for the system with 100 air blocks. Comparing these two diagrams we find that the air blocks are very strong scatterers and thus as few as only two air blocks are enough to determine the ranges of band gaps and pass bands. If the localization effect of AC waves in model 3 is mainly determined by the multiple scattering of AC waves between pairs of air blocks, then one would expect that for a system with 100 air blocks the transmission $T_{N=100}$ in the band gaps can be approximated by $T_{N=2}^{50}$, here $T_{N=2}$ refers to the transmission rate for two air blocks illustrated in 6(a). We indeed observed this result in Fig. 6(c). When randomness is not very large, this local effect explains why the phase averaging process in model 3 is so inefficient that the randomness cannot modify the LE much in the band gaps.

IV. CONCLUDING REMARKS

In this paper we studied the statistics of localization properties in one-dimensional layered systems. Luapunov exponent and its variance are compared for three chosen models. We find that the band structures of the corresponding periodic systems influence the localization properties much if the impedance contrast between neighboring layers is not close to 1. In general the single parameter scaling is not very accurate and more model-dependent parameters should be included in the detailed descriptions of localization behaviors.

ACKNOWLEDGEMENT

The work received support from National Science Council (No. NSC89-2611-M008-002 and NSC89-2112-M008-008).

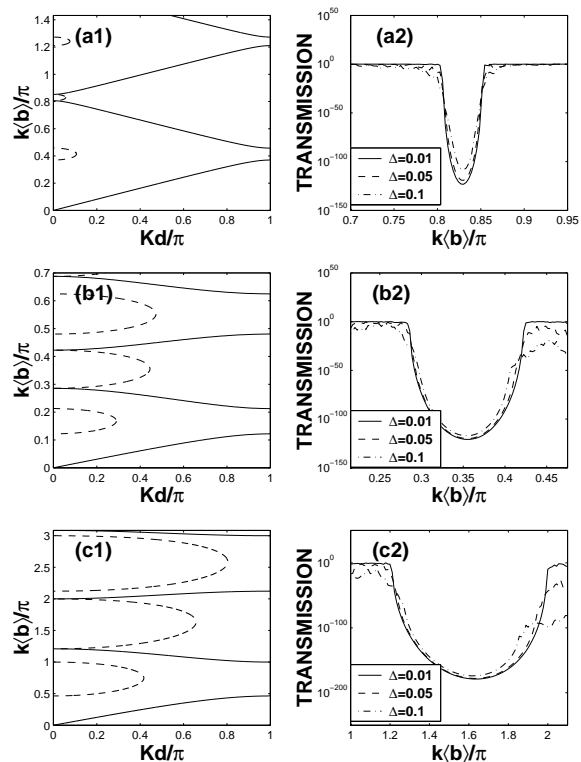


FIG. 1. Band structures (solid lines) and transmission curves for the three models discussed in this paper. (a1) and (a2) are for the first model. (b1), (b2) are for the second model. (c1) and (c2) are for the third model. The broken lines in (a1)-(c1) represent the inverse penetration depth $\text{Im}(K)$.

-
- [1] P. W. Anderson, Phys. Rev. **109**, 1492 (1958).
 - [2] V. Baluni and Willemssen, Phys. Rev. **A 31**, 3358 (1985).
 - [3] C. M. Soukoulis, E. N. Economou, G. S. Grest and M. H. Cohen, Phys. Rev. Lett. **62**, 575 (1989).
 - [4] D. Sornette and O. Legrand, J. Acoust. Soc. Am. **92** (1992).
 - [5] A. R. McGurn, K. T. Christensen, F. M. Mueller, and A. A. Maradudin, Phys. Rev. B **47**, 13120 (1993).
 - [6] Z. Ye and A. Alvarez, Phys. Rev. Lett. **80**, 3503 (1998).
 - [7] Z. Ye, H. Hsu, E. Hoskinson, and A. Alvarez, Chin. J. Phys. **37**, 343 (1999).
 - [8] M. Asch, W. Kohler, G. Papanicolaou, M. Postel, and B. White, SIAM Review **33**, 519-625 (1991).
 - [9] C. H. Hodges and J. Woodhouse, J. Acoust. Soc. Am. **74**, 894 (1983).
 - [10] R. Dalichaouch, J. P. Armstrong, S. Schultz, P. M. Platzman and S. L. McCall, Nature, **354**, 53 (1991).
 - [11] P. W. Anderson, D. J. Thouless, E. Abrahams, and D. S. Fisher, Phys. Rev. B **22**, 3519 (1980).
 - [12] J. Sak and B. Kramer, Phys. Rev. B **24**, 1761 (1981).
 - [13] J. Flores, P. A. Mello, and G. Monsiváis, Phys. Rev. B **35**, 2144 (1987).
 - [14] Avraham Cohen, Yehuda Roth, and Boris Shapiro, Phys. Rev. B **38**, 12125 (1988).
 - [15] L. I. Deych, D. Zaslavsky and A. A. Lisyansky, Phys. Rev. Lett. **81**, 5390 (1998)
 - [16] L. I. Deych, A. A. Lisyansky, and B. L. Altshuler, Phys. Rev. Lett. **84**, 2678 (2000).
 - [17] Pi-Gang Luan and Zhen Ye, Phys. Rev. E **63**, 066611 (2001).

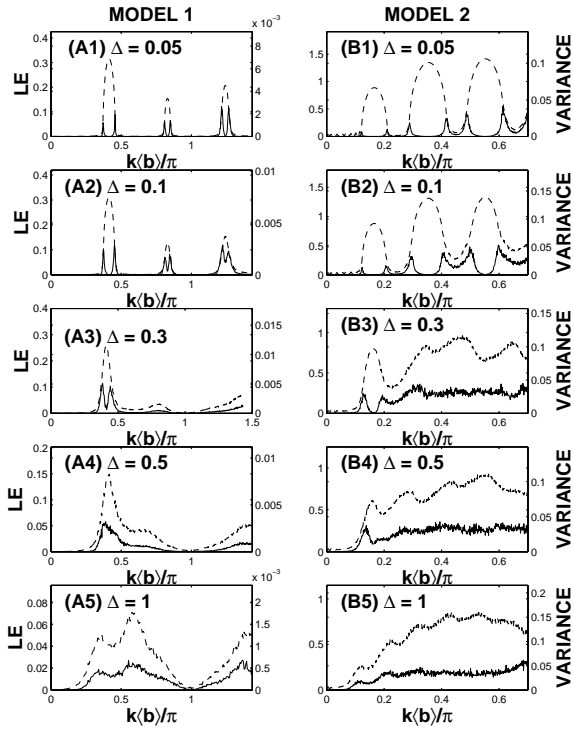
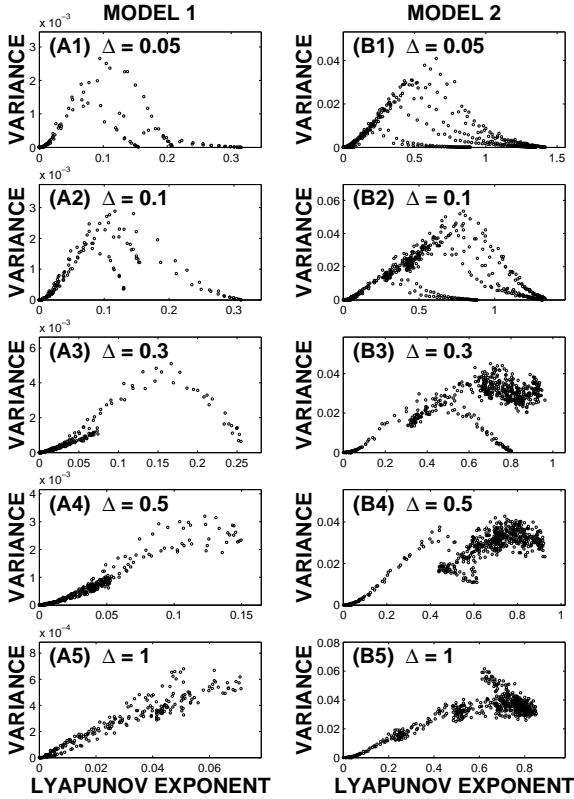


FIG. 2. LE (broken lines) and its variance (solid lines) for the first ((A1)-(A5)) and the second ((B1)-(B2)) models.

FIG. 3. $\text{var}(\gamma)$ versus γ for the first and the second models.



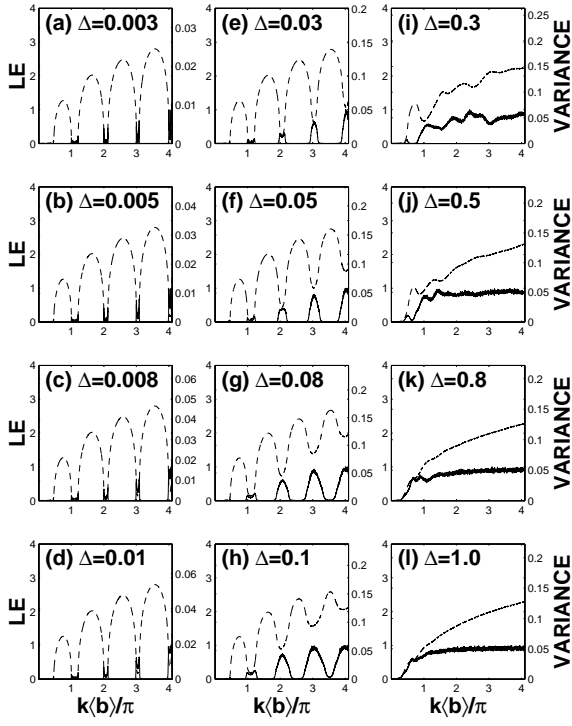


FIG. 4. Lyapunov exponent (broken lines) and its variance (solid lines) for the third model.

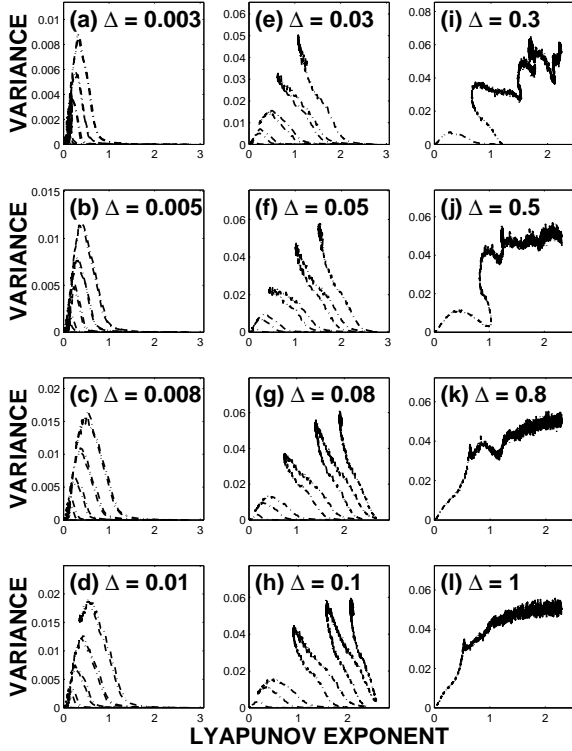


FIG. 5. $\text{var}(\gamma)$ versus γ for the third model.

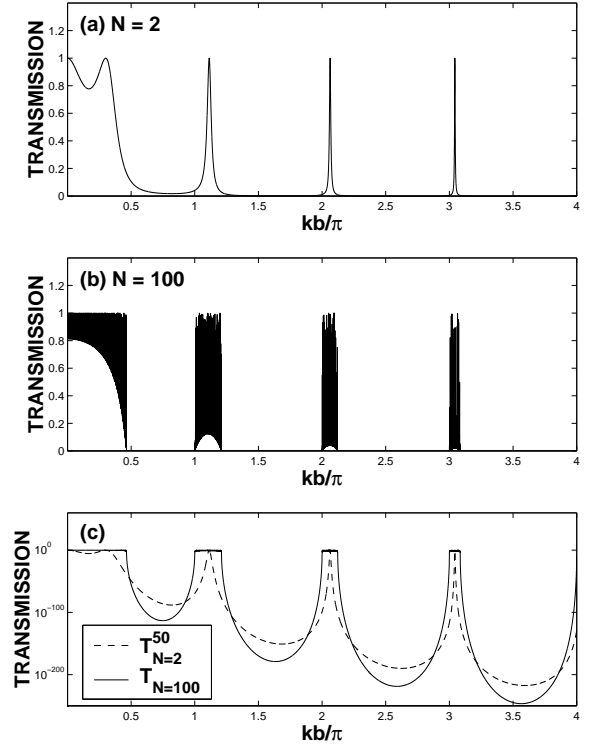


FIG. 6. Transmission vs dimensionless frequency for the third model. (a) Transmission for the $N=2$ system (two air blocks). (b) Transmission for the $N=100$ system (100 air blocks). (c) Comparison between $T_{N=2}^{50}$ (broken line) and $T_{N=100}$ (solid line).